plex $U(OC_3F_6H)_4(OC_2H_5)(HOC_2H_5)$, the quartet has broadened (fwhh ≈ 150 Hz) and shifted +16.3 ppm, while the secondary carbon has broadened (fwhh ≈ 100 Hz) and shifted +39.0 ppm (Figure 3F). Ethanol peaks were not definitively assignable, again presumably due to broadening, but could be the broad, weak absorption near 32 ppm and/or lie under the OC_3HF_6 absorption envelope. Thus, the fluoroalkoxide ligands appear to be equivalent by ^{13}C NMR at ambient temperature. The ^{19}F NMR spectrum at ambient temperature contained two broad peaks (fwhh = 37 and 56 Hz) of approximately equal intensity at +74.7 and +75.2 ppm (+75.4 ppm for ligand). At 70 °C, these peaks occur 2–3 ppm further upfield, have sharpened (fwhh ≈ 18 Hz), and have relative intensities of 1:3.8. When the solution is cooled to −35 °C the peaks broaden noticeably and remain about equal in intensity. As for $U(OC_4F_9)_4(OC_2H_5)(HOC_2H_5)$, some restricted rotation of CF_3 groups is indicated. The ^1H NMR spectrum contains no free ethanol peaks but does exhibit peaks at 2.0 ppm (fwhh ≈ 38 Hz) and 1.20 and 0.83 ppm (fwhh ≈ 8 Hz) attributable to coordinated ethoxy groups.

The ^{13}C NMR spectrum of C_6F_5OH (Figure 3B) contains four multiplets, occurring over the range 131.3–143.3 ppm, broadened 10–30 Hz by C–F spin–spin coupling. In $U(OC_6F_5)_5(HOC_2H_5)$ (Figure 3E), the ^{13}C NMR resonances have shifted to the range 129.6–157.7 ppm and the full widths at half-height have increased to 55–120 Hz. No peaks attributable to ethanol were assigned. Again, at room temperature the OR_f ligands seem to be equivalent by ^{13}C NMR. The ^{19}F resonances occurred in the range +155.6–158.7 ppm (fwhh = 27–54 Hz) compared to the sharp resonances in the range +160.4–165.5 ppm for the pentafluorophenol. The ^1H NMR spectrum showed no free ethanol to be present and had peaks at −3.6 ppm (fwhh ≈ 90 Hz) and −1.2 ppm (fwhh ≈ 20 Hz), which could be attributable to coordinated ethoxy groups.

Conclusions

The newly prepared uranium(V) fluoroalkoxide compounds are thermally stable, air-sensitive materials of low volatility. High-resolution ^{13}C NMR spectra are reported here for the first time for f^1 compounds and found to be useful for characterizing carbon-containing f^1 complexes. The ^{13}C spectra indicate temperature-dependent oligomeric structures in solution for $U(OC_2H_5)_5$ and $U(OC_6H_5)_5$. The fluoroalkoxide compounds are shown to be monomeric mixed-ligand complexes, whose NMR spectra indicate restricted CF_3 rotation.

Acknowledgment. This work was carried out under the auspices of the U.S. Department of Energy, Office of Basic Energy Sciences, Division of Chemical Sciences. Useful discussions with Dr. Gordon W. Halstead and Dr. Robert London on the latter stages of this work are gratefully acknowledged.

Registry No. $U(OC_6H_5)_5$, 86853-81-8; $U(OC_4F_9)_4(OC_2H_5)(HOC_2H_5)$, 86862-67-1; $U(OC_3F_6H)_4(OC_2H_5)(HOC_2H_5)$, 86853-83-0; $U(OC_6F_5)_5(HOC_2H_5)$, 86853-84-1; $Na[U(OC_2H_5)_6]$, 64653-58-3; $U(OC_2H_5)_5$, 10405-34-2; $U(OCH_3)_5$, 83178-45-4; $UF_3(OC_2H_5)_2$, 86853-82-9.

Supplementary Material Available: Tables of infrared spectra of uranium(V) alkoxides and near-IR–visible spectra of $U(OC_2H_5)_5$ and $U(OC_6H_5)_2$ (2 pages). Ordering information is given on any current masthead page.

Contribution from the Chemical Physics Program, Washington State University, Pullman, Washington 99164

Magnetic Susceptibility and EPR Study of Bis(β-alaninium) Tetrabromocuprate(II)

ROGER D. WILLETT,* RAYMOND J. WONG, and MICHIKO NUMATA

Received February 10, 1983

The structural, magnetic, and EPR properties of bis(β-alaninium) tetrabromocuprate(II), $(\beta\text{-alaH})_2CuBr_4$, are reported. The salt crystallizes in a monoclinic space group, $I2/c$, with a = 7.661 (1) Å, b = 8.027 (1) Å, c = 24.295 (7) Å, and β = 92.49 (2)°. It contains two-dimensional layers of square-planar $CuBr_4^{2-}$ anions separated by the organic cations. The compound exhibits ferromagnetic intralayer interactions with J/k = 21.2 K. Three-dimensional ordering occurs at T_c = 10 K. Magnetization studies reveal the existence of an Ising type anisotropy, with the easy axis normal to the layers. A substantial rhombic component also exists. The EPR spectrum consists of a single exchange-narrowed line of axial symmetry with $g_\parallel$ = 2.044 and $g_\perp$ = 2.098. The EPR line widths are strongly temperature dependent with phonon modulation of the spin anisotropies being the principal source of line broadening.

Introduction

Two-dimensional square-planar magnets of the type $(RNH_3)_2CuX_4$ (X = Cl^-, Br^-) have been of current interest in the study of the low-dimensional magnetic systems,[1-5] as well as model systems for lipid bilayers.[6,7] These salts are characterized by strong, nearly isotropic, ferromagnetic intralayer exchange interactions (J) and a very small ratio of inter- to intralayer exchange couplings ($|J'/J| \approx 10^{-3}$–10^{-4}).[3] In the chloride salts, the intralayer coupling is typically of the order $J/k \approx$ 15–20 K with a small XY-like anisotropy. Both ferro- and antiferromagnetic interlayer exchange couplings have been reported.[2,3] The intralayer coupling is slightly larger for the bromide salt, $J/k \approx$ 20–25 K, and the small anisotropic component of the exchange is now Ising-like. A smaller rhombic component to the anisotropy is also present in both types of salts. A renewed interest in the bromide salts has arisen due to the recent observation of large *inter*layer exchange coupling in the alkyldiammonium analogues, $(NH_3R_nH_{2n}NH_3)CuBr_4$, n = 2–4.[8]

(1) Soos, Z.; McGregor, K. T.; Cheng, T. T. P.; Silverstein, A. J. *Phys. Rev. B: Solid State* **1977**, *16*, 3036.
(2) Estes, W. E.; Losee, D. B.; Hatfield, W. E. *J. Chem. Phys.* **1980**, *72*, 630.
(3) de Jongh, L. J.; Miedema, A. R. *Adv. Phys.* **1974**, *23*, 1.
(4) Hagen, H.; Reimann, H.; Schmocker, U.; Waldner, F. *Physica B+C (Amsterdam)* **1977**, *86-88B+C*, 1287.
(5) Dupas, A.; Le Dang, K.; Renard, J.; Veilet, P.; Daoud, A.; Perret, R. *J. Chem. Phys.* **1970**, *65*, 4099.
(6) Kind, R.; Plesko, S.; Arend, H.; Blinc, R.; Zcks, B.; Seliger, J.; Lozar, B.; Slak, J.; Levstik, C.; Zagar, V.; Lahajnar, G.; Milia, F.; Chapus, G. *J. Chem. Phys.* **1979**, *71*, 2118.
(7) Needham, C. F.; Willett, R. D. *J. Phys. Chem.* **1981**, *85*, 3385.

0020-1669/83/1322-3189$01.50/0

Table I. Positional and Thermal Parameters for $(\beta\text{-alaH})_2CuBr_4$

atom	x^a	y^a	z^a	$\beta_{11}{}^a$	$\beta_{22}{}^a$	$\beta_{33}{}^b$	$\beta_{12}{}^a$	$\beta_{13}{}^a$	$\beta_{23}{}^a$
Cu	0	0	0	65 (4)	95 (5)	104 (5)	−25 (3)	−2 (1)	−1 (1)
Br(1)	241 (2)	297 (2)	995 (1)	127 (4)	124 (3)	118 (3)	−15 (2)	−5 (1)	−1 (1)
Br(2)	2324 (2)	2017 (2)	99 (1)	75 (3)	114 (3)	164 (4)	−30 (2)	−2 (1)	0 (1)
O(1)	3710 (14)	1898 (14)	3017 (4)	215 (28)	141 (21)	172 (23)	−44 (19)	−29 (6)	11 (6)
O(2)	2061 (15)	188 (13)	2495 (5)	210 (26)	138 (21)	161 (22)	−22 (18)	−30 (6)	1 (6)
N	273 (14)	4482 (16)	896 (5)	118 (25)	164 (27)	143 (26)	−30 (21)	−10 (7)	−5 (7)
C(1)	−207 (19)	5662 (21)	1337 (6)	123 (30)	199 (35)	101 (26)	50 (26)	1 (8)	0 (8)
C(2)	1310 (19)	6002 (20)	1750 (6)	158 (34)	138 (29)	109 (28)	12 (25)	−6 (8)	0 (8)
C(3)	1808 (19)	4482 (20)	2919 (7)	93 (27)	132 (30)	149 (32)	16 (25)	−1 (8)	−3 (8)

[a] Parameters multiplied by 10^4. [b] Parameters multiplied by 10^5.

Despite the similarities of the bulk magnetic properties of the chloride and bromide salts in this series, the relaxation properties, as measured by the EPR line widths, are very dissimilar. In particular, the room-temperature line widths of the bromides are generally 1 order of magnitude larger than those of the chlorides. The same is true of the temperature dependence of the line widths. In addition, the two types of salts show different types of angular dependence. For this reason, we have undertaken a detailed study of the structural, magnetic, and EPR characteristics of a new member of this series, $(\beta\text{-alaH})_2CuX_4$, where β-alaH ≡ $COOHCH_2CH_2NH_3^+$, the β-alaninium cation.[9]

The EPR behavior of low-dimensional magnetic systems has been of particular interest in the past decade. For a simple three-dimensional system with only isotropic exchange, it is well-known that the dipolar line width is narrowed by exchange. In addition, recent EPR studies on low-dimensional systems have indicated that spin diffusion can enhance the $q = 0$ Fourier component of the secular portion of the spin correlation function and lead to non-Lorentzian line shape and, for two-dimensional systems, a $(3\cos^2\theta - 1)^2$ angular dependence of the line width, where θ is the angle between the normal to the layer and the magnetic field.[10] These effects have been particularly observed for the quasi-2d Mn^{2+} crystals, which have very small spin–orbit coupling, and the main perturbation is from the dipolar interaction of the paramagnetic ions. In the copper salts, the anisotropic exchange interactions also act as perturbations, causing the broadening of the EPR line width and producing a simpler line width anisotropy.[1]

The intralayer interactions in these systems may be described by the spin Hamiltonian

$$\mathcal{H} = -2J\sum\vec{S}_i\cdot\vec{S}_j + D\sum S_i^z S_j^z + E\sum(S_i^x S_j^x - S_i^y S_j^y) + \sum\vec{d}\cdot\vec{S}_i\times\vec{S}_j \quad (1)$$

where the sums are over the nearest-neighbor pairs in the layer, D and E represent the symmetric anisotropy components of the isotropic exchange constant, J, and $\vec{d}$ is the antisymmetric exchange term. In a previous paper,[9] we have given details of the properties of the $(\beta\text{-alaH})_2CuCl_4$ system. The interesting properties of this system are related to a combination of two factors: a relatively large interlayer distance and hence very small interplane coupling and a large intralayer Cu–Cu distance, leading to an unusually small value of J. Magnetization studies below $T_c = 6.5$ K showed that the easy axis of magnetization was parallel to the crystallographic a axis, e.g. in the plane of the layer. The hard axis is normal to the layer. It was found that $J/k = 13.6$ K, $D = 850$ Oe, and $E = 150$ Oe. Thus, the chloride salts have an XY-anisotropy, with a rather small in-plane anisotropy. The value of D is considerably smaller than other layer copper chloride salts, a direct consequence of the small value of J, since D is usually estimated to be of the order $D \approx (\Delta g/g)^2 J$. The EPR spectrum of $(\beta\text{-alaH})_2CuCl_4$ was unique in the $(RNH_3)_2CuCl_4$ series of salts, in that the contributions of the exchange anisotropies were particularly subdued, allowing the observation of spin diffusion behavior.

As an attempt to study in more detail how the bromide ligands affect the magnetic properties in these compounds, the $(\beta\text{-alaH})_2CuBr_4$ salt was synthesized and the magnetic properties as well as the EPR study of the salt are reported in this paper. The differences of the magnetic behavior and the EPR line widths between the chloride and the bromide will be discussed.

Table II. Bond Distances and Angles for $(\beta\text{-alaH})_2CuBr_4$

atoms	dist, Å	atoms	angles, deg
	Copper–Bromide Network		
Cu-Br(1)	2.429 (1)	Br(1)-Cu-Br(2)	90.43 (5)
Cu-Br(2)	2.444 (1)	Br(1)-Cu-Br(2)[a]	88.57 (5)
Cu-Br(2)[a]	3.172 (1)	Br(2)-Cu-Br(2)[a]	91.37 (5)
		Cu-Br(2)-Cu[a]	167.53 (4)
	β-Alaninium Cation		
N-C(1)	1.49 (2)	N-C(1)-C(2)	111.9 (11)
C(1)-C(2)	1.54 (2)	C(1)-C(2)-C(3)	112.1 (13)
C(2)-C(3)	1.50 (2)	C(2)-C(3)-O(1)	124.6 (15)
C(3)-O(1)	1.19 (2)	C(2)-C(3)-O(2)	113.1 (14)
C(3)-O(2)	1.35 (2)	O(1)-C(3)-O(2)	122.2 (15)
O(1)-O(2)[b]	2.70 (1)	C(3)-O(1)-O(2)[b]	107.8 (9)
	Nitrogen–Bromine Hydrogen-Bonding Interactions		
N-Br(1)	3.37 (1)	Br(1)-N-Br(2)[c]	129.8 (14)
N-Br(2)[c]	3.42 (1)	Br(1)-N-Br(2)[d]	72.4 (13)
N-Br(2)[d]	3.47 (1)	Br(2)[c]-N-Br(2)[d]	99.8 (12)
		C(1)-N-Br(1)	125.5 (19)
		C(1)-N-Br(2)[c]	100.8 (17)
		C(1)-N-Br(2)[d]	122.9 (18)

[a] Coordinates transformed by $^1/_2 - x, -^1/_2 + y, -z$. [b] Coordinates transformed by $^1/_2 - x, ^1/_2 - y, ^1/_2 - z$. [c] Coordinates transformed by $^1/_2 - x, ^1/_2 + y, -z$. [d] Coordinates transformed by $-^1/_2 + x, ^1/_2 - y, z$.

Crystal Structure Determination

The compound is prepared by slow evaporation of a dilute HBr solution containing stoichiometric quantities of β-alanine and $CuBr_2$. The salt crystallized as deep purple, almost opaque crystals. Lattice constants, obtained from the accurate centering of 12 high-angle reflections, are $a = 7.761$ (1) Å, $b = 8.027(1)$ Å, $c = 24.295$ (7) Å, and $\beta = 92.49$ (2)°. Systematic extinctions ($h + k + 1 \neq 2n$ for hkl, and $l \neq 2n$ for $h0l$) defined the monoclinic space group $I2/c$, with $\rho_{calcd} = 3.05$ for $Z = 4$. Intensity data were collected on an automated Picker diffractometer with Mo Kα radiation. A total of 2348 reflections were measured of which 1278 had intensity greater than $3\sigma(I)$, where $\sigma^2(I) = (\text{total count}) + 0.05^2\,(\text{net count})^2$. The observed intensities were corrected for absorption. Least-squares refinement with anisotropic thermal parameters yielded a conventional R value of 0.092 for reflections with $F > 3\sigma$. No attempt was made

(8) Snively, L. O.; Haines, D. N.; Drumheller, J. E. *Phys. Rev. B: Condens. Matter* **1982**, *26*, 5245.
(9) Willett, R. D.; Jardine, F. H.; Rouse, I.; Wong, R. J.; Landee, C. P.; Numata, M. *Phys. Rev. B: Condens. Matter* **1981**, *24*, 5372.
(10) Richards, P. M. In "Local Properties at Phase Transitions"; K. A. Muller, Ed.; North-Holland Publishing Co.: Amsterdam, 1976; p 539.

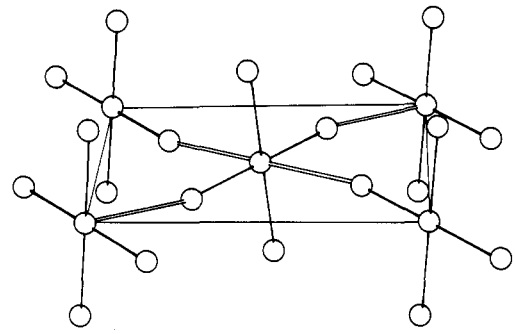

Figure 1. Illustration of the copper–halide layer structure in $(NH_3C_2H_4COOH)_2CuBr_4$. The *a* axis is horizontal, and the *c* axis is vertical.

to locate the hydrogen atoms. This, coupled with the propensity of copper(II) bromides to photodecompose, gives rise to the unusually high *R* value. All programs were from the Washington State University Crystallographic Library. The positional and thermal parameters are listed in Table I. The bond lengths and bond angles with standard deviations are listed in Table II.

Structural Results

This study represents the first single-crystal structure determination reported for a $(RNH_3)_2CuBr_4$ salt. The structure is strictly isomorphous with the corresponding chloride salt, as was anticipated. The copper–halide layer is depicted in Figure 1. Several comparisons between the two salts are worth making, however, as they have an impact on the magnetic properties. The increased ionic radii of the bromide ion over that of the chloride ion (1.95 vs. 1.80 Å) leads to an increase of the short Cu–X distances (heavy bonds, Figure 1) by an average of 0.14 Å. However, the long Cu–X distance (lighter bonds, Figure 1) only increased by 0.10 Å. The *intralayer* Cu–Cu distance is basically determined by the sum of these two distances. In $(\beta\text{-alaH})_2CuCl_4$, the *intralayer* Cu–Cu distance was unusually large (5.354 Å), 0.05–0.10 Å longer than in the simple $(RNH_3)_2CuCl_4$ salts.[11] This is presumably due to the steric bulk of the β-alaninium dimer as contrasted with the simpler aliphatic ammonium ions. Since there is a general correlation between metal–metal distance with the magnitude of the exchange interaction,[12] this larger distance is the cause of the low value of *J* in the chloride salt. Because there is only a small increase in the long Cu–Br distance, the intralayer Cu–Cu distance in the bromide salt (5.582 Å) is comparable to that of the other bromide salts.[3] Thus, it is anticipated that the exchange interaction on the bromide will be more nearly normal. It is also to be noted that there is essentially no change in the bridging bond angle (167.82° in the chloride vs. 167.53° in the bromide).

Magnetic Data

The magnetic susceptibilities of both powder and single-crystal samples were measured with a PAR vibrating-sample magnetometer. The data of 156.4 mg of a powder sample of the salt were taken at 5137 Oe over the temperature range 4–150 K. Single-crystal data were also taken with use of samples of 34.5 and 23.6 mg with an applied field of 56 and 103 Oe along each of the crystallographic axes. All experimental moments were corrected for background with use of a bare sample rod, and all susceptibility data were corrected for the diamagnetism of constituent atoms. Finally magnetizations vs. applied field along each axis were measured at 4.2 K.

EPR Experiments

The EPR spectra of single crystals carefully aligned by X-ray techniques were taken at room temperature and liquid-nitrogen

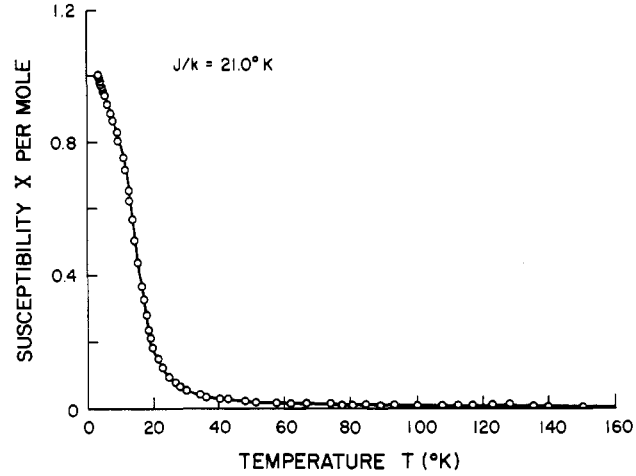

Figure 2. Powder susceptibility for $(NH_3C_2H_4COOH)_2CuBr_4$ at H = 5094 Oe. The solid curve is the fit to the high-temperature series expansion for a two-dimensional spin $^1/_2$ ferromagnet.

temperature on both a Varian E-3 spectrometer fitted with a goniometer (for the 9-GHz measurement) and a homemade Q-band spectrometer (36 GHz) equipped with a rotating magnet. The temperature dependence of line width over the range of 77–300 K was studied with a Varian E-9 spectrometer equipped with a temperature controller. Spectra were recorded with the applied field along each crystallographic axis for the temperature dependence experiment. Similar measurements were carried out on $(C_2H_5NH_3)_2CuBr_4$ and $(C_3H_7NH_3)_2CuBr_4$. The EPR spectra are single lines at all angles with broad line widths (400–600 Oe at 300 K and 30–50 Oe at 77 K), with the line shapes being nearly Lorentzian. The line widths reported here are peak-to-peak line widths measured from the first-derivative signal.

Magnetic Results

The susceptibility data of the powder sample are shown in Figure 2. A plot of $1/\chi_M$ vs. T gives a Curie–Weiss constant of 28.5 ± 0.5 K based on data above 50 K. The average g value obtained from this data corresponds to 2.10 for a spin $^1/_2$ system. The behavior of the χ_M–T curve clearly shows that the predominant interaction is ferromagnetic. The data above 30 K were fit to the high-temperature series expansion for a spin $^1/_2$ Heisenberg square ferromagnet[13] to obtain a value of J/k = 21.2 K. The average EPR g factor of 2.080 was used.

Single-crystal magnetic data, corrected for demagnetization effects (Figures 3 and 4), reveal the presence of long-range order as well as considerable anisotropy at low temperature. The value of T_c is estimated as 10.0 ± 0.5 K from the temperature of the maximum slope of $\chi_\perp$. The single-crystal magnetization data (Figure 4) show no evidence of a spin flop or metamagnetic phase transition in the field range $50 \leq H \leq 10\,000$ Oe. Thus, the interlayer coupling is likely ferromagnetic, although a transition could occur below 50 Oe, the lower limit of our magnet system. The magnetization data show a predominant Ising anisotropy with the easy axis parallel to c^* (e.g., normal to the layer). However, the low-temperature susceptibility data (Figure 3) are indicative of rhombic anisotropy with the hard axis parallel to *a*. Quantitatively, the anisotropy can be characterized in terms of the fields $H_a^{out} = DH_{ex}$ and $H_a^{in} = EH_{ex}$, where $H_{ex} = 2zJS/g\beta$. These fields can be estimated from the differences in the intersections of the linear extrapolation of the low- and high-field portions of the magnetization curves along the *a*, *b*, and c^* crystallographic axes.[14] Alternatively, they can be obtained from the sus-

(11) Steadman, J. P.; Willett, R. D. *Inorg. Chim. Acta* **1970**, *4*, 367.
(12) de Jongh, L. J.; Block, R. *Physica B+C (Amsterdam)* **1975**, *79B+C*, 568.
(13) Baker, G. A.; Gilbert, H. E.; Eve, J.; Rushbrooke, G. S. *Phys. Lett. A* **1967**, *25A*, 207.
(14) de Jongh, L. J.; van Amstel, W. D.; Miedema, A. R. *Physica (Amsterdam)* **1972**, *58*, 277.

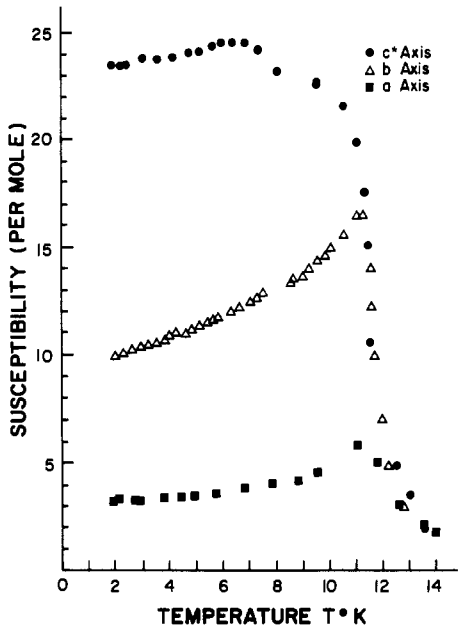

Figure 3. Single-crystal susceptibility data for $(NH_3C_2H_4COOH)_2CuBr_4$ at H = 103 Oe.

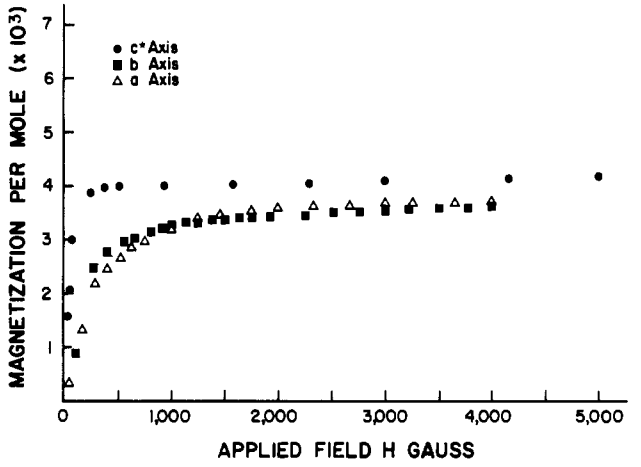

Figure 4. Single-crystal magnetization data for $(NH_3C_2H_4COOH)_2CuBr_4$ at 4.2 K.

ceptibilities along the intermediate and hard axes.[14] The former yields H_a^{out} = −600 Oe and H_a^{in} = −300 Oe, confirming the existence of a rhombic type anisotropy. The susceptibility results yield H_a^{out} = −650 Oe and H_a^{in} = −200 Oe, in adequate agreement.

These results may be compared (Table III) with those for $(\beta\text{-alaH})_2CuCl_4$, along with two other representative systems, $(C_2H_5NH_3)_2CuX_4$ and $(C_3H_7NH_3)_2CuX_4$, X = Cl^- and Br^-.[6] A number of trends are discernible. First, the isotropic exchange constant for $(\beta\text{-alaH})_2CuBr_4$ is the same order of magnitude as in the other bromide salts. This is consistent with the fact that the intralayer Cu–Cu distance is nearly the same in these three bromide salts. In an examination of the anisotropy fields, it is noted, as has been recognized previously, that the anisotropy changes from XY-like to Ising-like upon replacement of Cl^- by Br^-. Also the magnitude of the out-of-plane anisotropy is substantially smaller in the $(\beta\text{-alaH})_2CuX_4$ salts than in the other salts. This was expected for the chloride salt (because of its low value of J) but unanticipated for the bromide salt. The in-plane anisotropy, on the other hand, is larger for the $(\beta\text{-alaH})_2CuX_4$ salts than for the other salts in the $(RNH_3)_2CuX_4$ series.

Table III. Anisotropic Exchange Fields and Exchange Parameters in Selected Salts

	magnetic anal.			EPR anal.	
	J/k, K	H_A^{in}, Oe	H_A^{out}, Oe	d_x/d_y	R_A
$(\beta\text{-alaH})_2CuCl_4$[a]	13.8	150	+850 (XY)	1.3	1.60
$(\beta\text{-alaH})_2CuBr_4$	21.2	−300	−600 (Ising)	1.0	0.68
$(C_2H_5NH_3)_2CuCl_4$[b]	18.6	80	+1500 (XY)	1.0	2.5
$(C_2H_5NH_3)_2CuBr_4$[b]	19.0	170	−2300 (Ising)	1.0	1.1
$(C_3H_7NH_3)_2CuCl_4$[b]	16.0	50	+1440 (XY)	1.0	2.0
$(C_3H_7NH_3)_2CuBr_4$[b]	21.3	260	−2600 (Ising)	1.0	0.75

[a] Reference 9. [b] Reference 3.

EPR g-Tensor Analysis

The angular variation of the EPR g value shows a simple $g^2 = g_\parallel^2 \cos^2\theta + g_\perp^2 \sin^2\theta$ dependence with $g_\parallel$ = 2.044 and $g_\perp$ = 2.098. Here, and subsequently, we use a spherical coordinate system with angles ϕ and θ defined relative to an x, y, z coordinate system with $x \| a$, $y \| b$, and $z \| c^*$. No in-plane anisotropy is observed. This is the usual behavior for $(RNH_3)_2CuX_4$ salts. The only exception reported to date is for $(\beta\text{-alaH})_2CuCl_4$, where a small ϕ dependence was also noted with g_a = 2.171, g_b = 2.151, and g_{c^*} = 2.045. In view of the similarities of the structures of the chloride and bromide salts of β-alaH$^+$, and the large value for the in-plane anisotropy for both salts, this difference in angular variation of g values is puzzling.

The fact that the values of the g-tensor components are much smaller for the bromide than for the chloride deserves further comment. The reason for this can be seen from examination by the expression for the components of the g tensor in terms of the molecular orbital parameters.[15] Thus, we have

$$g_\alpha = 2.0023 + a(\lambda_M - b\lambda_L)/\Delta E_{d\text{-}d} + a'(\lambda_M + b'\lambda_L)/\Delta E_{CT} \quad (2)$$

where a, a', b, b' are coefficients that depend on the bonding between the metal and the ligand, λ_M and λ_L are the spin-orbit coupling parameters for the metal and the ligand, and $\Delta E_{d\text{-}d}$ and ΔE_{CT} are the d–d and charge-transfer transition energies. The various coefficients and $\Delta E_{d\text{-}d}$ change very little upon replacement of the chloride ligand by bromide. However, λ increases from 586 to 2273 cm^{-1} (λ_M for Cu^{2+} = −830 cm^{-1}) while ΔE_{CT} decreases from ~25 000 to ~16 000 cm^{-1}. The second term is always positive and is of the same order of magnitude for the two salts. In contrast, b' is of such a magnitude that the third term becomes negative for the bromide salt, while the change in ΔE_{CT} gives that term a larger contribution. Thus, the deviation of the g value from 2.0023 is smaller for the bromide even though there is an increase in ligand spin–orbit coupling.

Line Width Analysis and Anisotropy

In analyzing the EPR line width data for $(\beta\text{-alaH})_2CuBr_4$, we observe first (Figures 5 and 6) that, like the g tensor, the line widths show a simple $\cos^2\theta$ behavior over the temperature range of 78–300 K. No evidence of a ϕ dependence nor of a spin diffusive type of $(3\cos^2\theta - 1)^2$ behavior, similar to that observed in the corresponding chloride salt, is found. It is also noted that the line widths vary by 1 order of magnitude over the temperature range from 78 to 300 K. In contrast, the line widths vary only by a factor of 2 in the chloride salt. This is a general trend in $(RNH_3)_2CuX_4$ salts.[16] The linear de-

(15) Smith, D. W. *J. Chem. Soc. A* **1970**, 3108. Chow, C.; Chang, K.; Willett, R. D. *J. Chem. Phys.* **1973**, *59*, 2629.

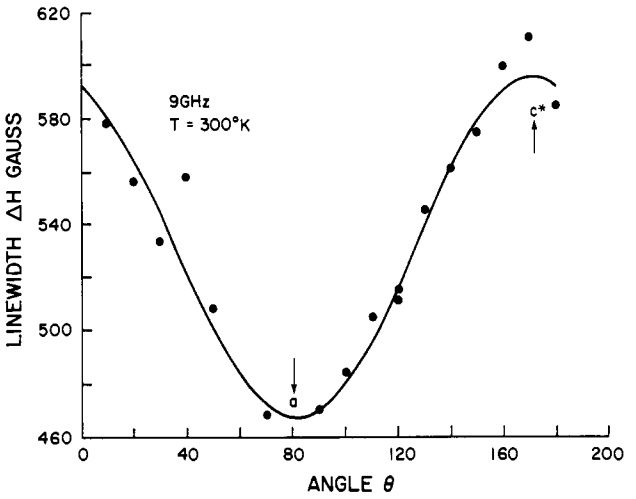

Figure 5. Angular dependence of the EPR line widths for $(NH_3C_2H_4COOH)_2CuBr_4$ at 300 K.

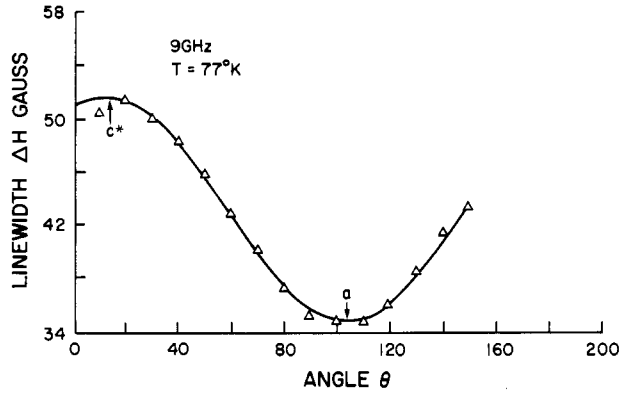

Figure 6. Angular dependence of the EPR line widths for $(NH_3C_2H_4COOH)_2CuBr_4$ at 77 K.

pendence on temperature (Figure 7) is reminiscent of that observed in copper formate by Seehra and Castner and can be explained in terms of phonon modulation of the antisymmetric exchange interaction.[17] We have treated this in detail in a separate paper[16] and shown that the larger temperature dependence of the bromide salts with respect to the chloride salts is a direct consequence of the larger spin–orbit coupling constant of the bromide ion. At this point we simply note that the extremely large temperature dependence makes it impossible to approximate ω_{eff} (vide infra) at 78 K by J/h, as was done for the chloride salt. Thus, quantitative estimates of the magnitude of the anisotropy of the exchange parameters cannot be made.

The analysis of the angular dependence of the line width will proceed in much the same manner as developed by Soos et al.[1] They have studied the EPR anisotropies of the $(PDA)CuCl_4$ and $(PTA)CuCl_4$ systems and concluded that line broadening results from the anisotropic exchange, D, and antisymmetric exchange, $\vec{d}$. The anisotropic and antisymmetric exchange terms act as short-time perturbations and obscure the anticipated low-dimensional effects. Thus, Soos et al. were not able to observe the spin diffusion effect on the line width and line shape. Instead, a simpler $\sin^2\theta$ angular dependence was observed. The anistropic line width was expressed as

$$\Delta H(\theta,\phi,T) = 2M_2(\beta J)/3^{1/2}\omega_{eff} \quad (3)$$

(16) Wong, R.; Willett, R. D. *J. Magn. Reson.* **1981**, *42*, 446.
(17) Seehra, M. S.; Castner, T. G. *Phys. Kondens. Mater.* **1967**, *7*, 185. Castner, T. G., Jr.; Seehra, M. S. *Phys. Rev. B: Solid State* **1971**, *4*, 38.

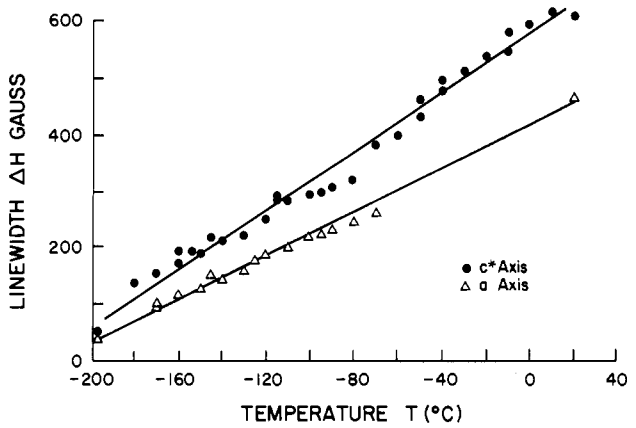

Figure 7. Temperature dependence of the EPR line widths for $(NH_3C_2H_4COOH)_2CuBr_4$ along the a and c^* axes.

where $M_2(\beta J)$, with $\beta = 1/kT$, is the temperature-dependent second moment arising from the anisotropic components of the exchange and ω_{eff} accounts for the spin–lattice relaxation contributions to the line widths. Using the explicit formulas developed by Soos et al., we have

$$\Delta H(\theta,\phi,T) = \frac{2}{3^{1/2}\omega_{eff}}\left\{[(M_2^A(\theta,\phi))F^A(\beta J)) + (M_2^S(\theta)(F^S(\beta J))]\frac{\chi_C}{\chi(T)}\right\} \quad (4)$$

where

$$M_2^A(\theta,\phi) = \frac{Zd_x^2(1+\sin^2\theta\cos^2\phi)}{16} + \frac{Zd_y^2(1+\sin^2\theta\sin^2\phi)}{16} + \frac{Zd_z^2(1+\cos^2\theta)}{16}$$

$$= \frac{Zd_y^2(2+\sin^2\theta)}{16} + Z(d_x^2-d_y^2)\frac{(1+\sin^2\theta\cos^2\phi)}{16} + Zd_z^2\frac{(1+\cos^2\theta)}{16} \quad (5)$$

$$M_2^S(\theta) = \frac{ZD^2(1+\cos^2\theta)}{8}$$

$F^A(\beta J)$ and $F^S(\beta J)$ account for the temperature dependence of the static correlation functions arising from the antisymmetric and symmetric exchange, respectively, and Z is the number of nearest neighbors.

We now apply this to the line width data for $(\beta\text{-alaH})_2CuBr_4$. From the fact that the line width depends only on θ, and not on the orientation of the field within the layer, it is concluded that $|d_x| = |d_y|$. From the values of ΔH(90,0,78 K) to ΔH(0,0,78 K) the anisotropy ratio, R_A, can be calculated, where

$$R_A = (d_x^2 + d_y^2)/(d_z^2 + fD^2)$$

with $f = F^S(\beta J)/F^A(\beta J) = 3.0$ for $(\beta\text{-alaH})_2CuBr_4$ at 78 K. It is found that $R_A = 0.68$ for the bromide salt at $T = 78$ K.

Table III compares these results with those for other chloride and bromide salts. It is seen that all of the bromides have a $(A + B\cos^2\theta)$ angular dependence, in contrast to the $(A + B\sin^2\theta)$ dependence of the chloride salts reported by Soos. This would indicate that the relative magnitudes of the d_x and d_y components are smaller for the bromide than the chloride. The quantitative analysis of the data bears this out, since $R_A = 0.68$ for $(\beta\text{-alaH})_2CuBr_4$ and 1.6 for $(\beta\text{-alaH})_2CuCl_4$. In the other chlorides this ratio is greater than 2, while it ranges between 0.75 and 1.1 for the bromides.

Table IV. Angular Dependence of EPR Line Widths for $(RNH_3)_2CuBr_4$ Salts at 77 K

compds	ΔH_{pp}, Oe	compds	ΔH_{pp}, Oe
$(\beta\text{-alaH})_2CuBr_4$	$49 + 14\cos^2\theta$	$(PA)_2CuBr_4$[a]	$97 + 28\cos^2\theta$
$(EA)_2CuBr_4$[a]	$111 + 20\cos^2\theta$	$(PDA)CuBr_4$[a]	$118 + 20\cos^2\theta$

[a] Reference 9.

Conclusions

The salt $(\beta\text{-alaH})_2CuBr_4$ has been shown to be a two-dimensional system with strong ferromagnetic intralayer coupling. The value of $J/k = 21.2$ K obtained is comparable that for to other $(RNH_3)_2CuBr_4$ salts. The exchange interaction is very nearly Heisenberg in nature, with only a small orthorhombic anisotropy. The easy axis is normal to the layer. Consistent with results on other $(RNH_3)_2CuX_4$ systems, the magnetic data indicate that the $(\beta\text{-alaH})_2CuX_4$ salts switch from a predominant XY anisotropy in the chloride salt to a predominant Ising anisotropy in the bromide salt. This changeover is probably a direct result of the reduction of single-ion anisotropy for the bromide salt with respect to the chloride salt. The value of $g_\perp - g_\parallel$, which contributes toward an XY-like anisotropy, is reduced from 0.116 for $(\beta\text{-alaH})_2CuCl_4$ to 0.054 for $(\beta\text{-alaH})_2CuBr_4$.

It has been shown that the angular dependence of the EPR line widths can be accounted for by the contributions of the magnetic anisotropies to the relaxation processes. Thus, the EPR behavior of the $(RNH_3)_2CuBr_4$ salts can be accounted for by the same formalism as proposed by Soos et al.[1] for $(RNH_3)_2CuCl_4$ salts. In an examination of the trends in the spin anisotropies as determined by the EPR measurements (Table IV), it is observed that $R_A(Br) < {}^1/_2R_A(Cl)$. The d_x and d_y components of the antisymmetric exchange would be expected to lead to an Ising-like anisotropy while the d_z component favors an XY anisotropy. The smaller value of R_A for the bromide salts would indicate that the exchange anisotropies should favor stronger XY anisotropy in $(RNH_3)_2CuBr_4$ salts. This is in direct contrast to the magnetic anisotropy measurements. Thus, the exchange anisotropies must make a smaller contribution to the total magnetic anisotropy than the single-ion anisotropy.

Acknowledgment. The assistance of Dr. C. P. Landee with magnetic measurements and D. R. Bloomquist with crystallographic measurements is gratefully acknowledged. This work was supported by a grant from the NSF.

Registry No. II, 77460-74-3.

Supplementary Material Available: A listing of observed and calculated structure factors (2 pages). Ordering information is given on any current masthead page.

Contribution from Ames Laboratory—DOE[1] and the Department of Chemistry, Iowa State University, Ames, Iowa 50011

A Photoelectron Spectroscopic Study of the Zirconium Monohalide Hydrides and Zirconium Dihydride. Classification of Metal Hydrides as Conventional Compounds

JOHN D. CORBETT* and HENRY S. MAREK

Received December 28, 1982

Core and valence (Al Kα, He I) spectra are reported for $ZrH_{1.90}$ and for the layered $ZrXH_{0.5}$ and ZrXH (X = Cl, Br), in which hydrogen occurs in tetrahedral interstices between double metal layers. Significant Zr–H covalency is suggested by the valence XPS results for ZrXH and is very evident with $ZrH_{1.9}$, where a strong band appears at 4.8 eV. The very similar UV spectra for the chloride and bromide series show the development of a sharp hydride band at ~5.4 eV together with appreciable changes in the metal-rich band near E_F. A general consideration is provided of the interrelationships between the title compounds and binary metallic compounds formed by hydrogen and by other non-metals, halogen especially. These metal hydrides generally exhibit a consistent and well-defined pseudohalide-like anionic state with a binding energy 5–6 eV, a crystal radius of ~1.10 Å, and significant M–H covalency. Fluoride-like structures are appropriate for the hydrides on the basis of anion sizes, but isostructural pairs are found mainly with some tripositive metals because of the poor oxidizing power of H_2 and, possibly, the greater covalency of hydride. The behavior of hydrogen is regular in the sense that it appears to oxidize the metal in reduced compounds of other non-metals only to the same oxidation state that is achieved in the highest binary metal hydrides.

Introduction

Traditionally the metallic hydrides have been viewed as being somewhat separate and apart from the rest of chemistry, either with regard to the salt-like hydrides vs. halides, oxides, etc. or with respect to metal–metal-bonded and often metallic compounds containing other non-metals. Indeed, the metallic hydrides along with some other metal-rich compounds of the second-period non-metals have often been classified as "interstitial", a particularly inept term in many cases in view of the substantial structural and volume changes associated with their formation. Recent years have seen considerable gains in examples and understanding of metallic halides, chalcogenides, and pnictides and their interrelationships with both metals and "normal" (insulating or semiconducting) compounds. The chemistry of the metallic hydrides and their relationship to these other metallic phases have been pursued somewhat less intensively, and the time appears to be appropriate to consider whether a distinction in kind is really warranted. The properties of binary and ternary compounds of zirconium and neighboring elements with hydrogen, halide, and other non-metals are particularly instructive in establishing that the hydrides exhibit a plausible anion state with a set of properties nonlinearly related to the analogous halides.

The zirconium monohalides ZrCl and ZrBr[2] provide good representations of two-dimensional metals (including interstices) as they consist of four-layer slabs in which pairs of

(1) Operated for the U. S. Department of Energy by Iowa State University under Contract No. W-7405-Eng-82. This research was supported by the Office of Basic Energy Sciences, Materials Sciences Division.

(2) Struss, A. W.; Corbett, J. D. *Inorg. Chem.* **1970**, *9*, 1373.

0020-1669/83/1322-3194$01.50/0